Study the Microstructural Characteristics and Mechanical, Physical and Abrasive Wear Properties of 2014 Al-TiC metal Matrix Composite (MMC) Synthesized by in-Situ Technique and Compare their properties with base Alloy

Suraj Kumar Singh[1], Prof. Krishna Bhushan Patel[2]
[1, 2] RAJEEV GANDHI PROUDYOGIKI MAHAVIDYALAYA, BHOPAL (M.P.)

Abstract- *This dissertation's primary objective is to investigate the microstructural characteristics, and mechanical, physical, and abrasive wear parameters of the 2014 Al-TiC metal matrix composite (MMC), created using the in-situ method. Comparing these characteristics to those of the base alloy is a crucial goal. This chapter introduces the different pertinent elements pertaining to the topic of the current study, including composites, wear, and other critical mechanical qualities, in keeping with the chapter's goal.*

Keywords- MMC, composite material, sliding distance etc.

I. INTRODUCTION

1.1 Composite Materials

Two different materials that are physically separated by an interface are combined to create composites, which are typically made of manmade materials but can also occasionally be found in nature, like wood. In comparison to their constituent components, these composites have improved characteristics. The reinforcing phase and the matrix phase are two separate stages that make up a composite. The matrix phase contains the reinforcing phase, which is important to giving the composite its strength. Particles, fibres, and sheets are some of the different types of reinforcing phases that can be used in composites, while polymers, ceramics, and metals can be used as matrix materials [1]

1.2 Processing of Metal Matrix Composites

Two techniques—in-situ and ex-situ—can be used to integrate the dispersoid phase, which improves the characteristics of the composite [16]. The dispersoid phase is produced by the matrix ingredients in the in-situ approach. This method has many benefits, including better uniformity of the dispersoid phase distribution in the matrix, enhanced interfacial bonding between the dispersoid and matrix, and precise control over the size and composition of the reinforcement. As a result, in-situ inclusion produces composites with better characteristics than ex-situ techniques.

1.3 Wear

Wear is the term used to describe the slow removal of material from a solid body's surface When it comes to engine bearings, wear happens when the surface of the bearing gradually loses bearing material owing to sliding friction. The friction between the two interacting materials causes a variety of physical and chemical processes, which together make up the wear process. These include procedures like welding, melting, and chemical reactions, as well as micro-cutting, micro-ploughing, plastic deformation, cracking, and fracturing. Abrasive wear, sticky wear, fatigue wear, corrosive wear, and erosive wear are just a few examples of the various forms of wear that can occur. The performance and longevity of the associated components are impacted by these numerous wear mechanisms, which also contribute to the deterioration and material loss from the surfaces in contact.

II. LITERATURE REVIEW

Introduction

‘

Due to its distinct combination of desirable qualities, including as superior corrosion resistance, low density, and great mechanical properties, aluminium has recently received major global study attention. Aluminium composites' thermal characteristics, such as metallic conductivity and the capacity to adjust the coefficient of expansion to values near to zero, expand the scope of their possible uses in the aerospace and avionics sectors. Because of this, entire families of lightweight composites that were previously thought to be unfeasible are now either available or close to commercialization

2.1 Preparation of Composites

Hybrid composites—those incorporating two or more reinforcements—have sparked a great deal of attention in the area of MMCs because of their potential for enhanced mechanical qualities.

Several studies on hybrid MMCs have been undertaken, and the findings are intriguing. Karthick et al. [30] developed hybrid composites reinforced with Al2O3 and SiC, and they found that the composite with 8 weight percent SiC and 5 weight percent alumina had the highest microhardness. Due to their optimum properties of equiaxed fine grains, evenly distributed fine in-situ Al4SiC4 particles, and Al3Ti nano-precipitates, the composites with 4 vol% TiC and 4 vol% SiC that Show et al. [31] tested had high strength. Ramnath et al. [32] studied hybrid MMCs made of aluminium alloy, alumina, and boron carbide and found that the addition of hard ceramic phases boosted impact strength, but that non-uniform particle distribution, agglomeration, and porosity affected tensile and flexural strength.

In composites with additional SiC and mixed reinforcements (SiC and graphite), Aatthisugan et al. [33] found higher tensile strength and hardness due to the presence of hard ceramic reinforcements and homogeneous particle distribution. Using SEM imaging, Inside the magnesium matrix, Prakash et al. [34] found flake-like graphite and evenly scattered, sharp-edged SiC particles. Using nanosized Al2O3 and microsized SiC to make hybrid MMCs, Kannan and Ramanujan [35] noted that this led to a higher porosity due to agglomeration and clustering, which hampered molten matrix flow. Raw carbon fibre (CF), hydrazine-reduced graphene (G), and graphene oxide (GO) powders were blended, however, no diffraction peaks of CF/G were found when Zhang et al. [36] employed XRD to evaluate the mixture, possibly due to their low concentration.

2.2 Abrasive Wear Behaviour

Three important stages or trends in the development of wear modelling models have been noted over time: empirical equations, the contact mechanics method, and the failure mechanics approach [71]. We'll concentrate on D. Tabor's traditional theory of wear in this conversation. According to D. Tabor's hypothesis, surface imperfections operate as bridges between two bodies, greatly reducing the real contact area between them while increasing the apparent contact area [71]. In order to substantiate this assertion, Tabor carried out practical studies and referred to significant contributions to the field of contact mechanics, beginning with Hertz's theory of elastic deformation and the computation of contact area variance with load [72]. Conductance between crossed cylinders was further investigated by Bidwell [73]. On top of these foundations, Tabor et al. [71] investigated the actual area of contact between bodies, putting forth the theory that a rise in applied load would cause a rise in contact and conductance. Based on elastic and plastic assumptions, Tabor created two theoretical equations that predicted conductivity would be influenced by the cubed root and square root of the load, respectively. Using a crossed-cylinders apparatus, these hypotheses were confirmed, with the equation based on the assumption of plastic deformation displaying the strongest correlation. The authors' research supported Amonton's law of friction, which states that the total cross section of junctions and the necessary tangential force are inversely proportional [71].

III. PROBLEM IDENTIFICATION

The information that is now available indicates that many procedures are employed to create metal matrix composites (MMCs). The pathways of liquid and powder metallurgy, as well as mixtures of these processes, spray co-deposition, rheo-casting, compo-casting, gravity, and pressurized solidification procedures, are among these methods. There are two ways to incorporate the reinforcing phase into the alloy matrix: ex-situ and in-situ approaches.

Numerous material and test criteria have an impact on the wear characteristics of alloys when it comes to the wear response of materials. Alloy chemistry, microstructural characteristics, material processing stages, and parameters are examples of material-related parameters. The shape, size, characteristics, and distribution pattern of the dispersoid phase, as well as the kind of the matrix/particle interfacial interaction, are additional factors controlling wear response in the case of composites. The properties, shape, and size of the abrasive particles, the applied force, traversal speed, and distance are test criteria particular to abrasive wear. The method of testing the material is crucial, even for the same sliding distance. It's interesting to note that there is no clear pattern regarding how material and test parameters affect wear behaviour. This implies that the wear performance of materials needs to be examined on a case-by-case basis to assess their response more realistically.

In light of these findings, the objective of this work is to determine how the traversal distance, abrasive size, applied load, and test mode affect the wear characteristics of an aluminium alloy and its composites comprising ultrafine 5% and 10% TiC dispersoid particles. The effects of TiC reinforcement and its composition on wear behaviour are also investigated in the study. Wear rate, frictional heating, and friction coefficient are three important wear metrics that are examined. The findings are examined in relation to the type of harm done to the abrasive medium and the resistance offered by the reinforced TiC particles to the abrasive particles' penetrating action within the material system.

IV. EXPERIMENTAL SECTION

Process Flow Diagram

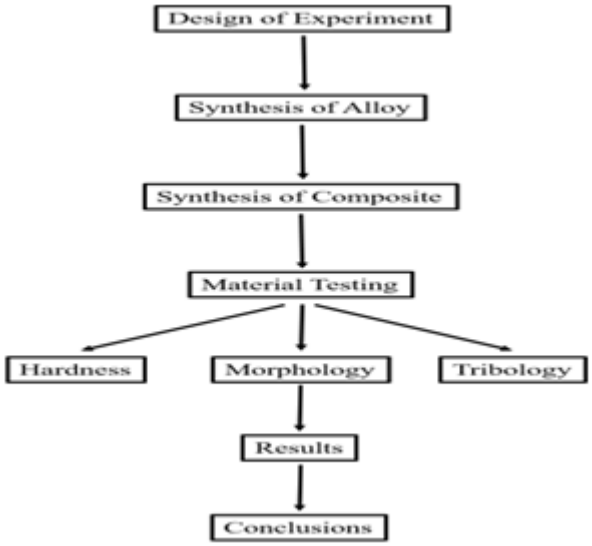

Figure 4.1 Flow chart of experimental work

4.1 Material Preparation

Liquid metallurgy was used to create the aluminum-based alloy and its in-situ composites, and graphite crucibles were used for melting. In a safe argon environment, melting was done in an electric resistance furnace. The 2014 Al alloy's required composition was achieved by melting a pure commercial aluminium ingot and adding 99.9% pure Mn, Mg, Cu, and Fe chips to produce nthe base alloy. Table 4.1 lists the precise chemical make-up of the synthesised alloys and composites. The melt received extensive stirring and degassing after the alloying components were added in the necessary weight percentages. Then, a permanent cast iron mould was heated before the aluminium alloy melt was put into it and let to cool.

Al-TiC composites with two distinct volume percentages of TiC were produced using the in-situ manufacturing method. In order to create the TiC phase, a reaction between a combination of Ti and C particles was introduced into the alloy melt during the operation. According to the intended 5 and 10 wt% TiC compositions, the elemental powders of Ti and C were added to the alloy melt while still warmed. After the reaction was finished, a mechanical stirrer spinning at 500 rpm was used to agitate the melt before it was put into a permanent die mould. Both the Al alloy and composites were poured at a temperature of 800 °C. The castings made were cylinder-shaped rods with a 10 mm diameter and 150 mm length. The processing flow chart for synthesizing the alloy and composite is illustrated in Fig. 4.1, while the melting facility and the resulting castings are presented in Fig. 4.2.

Table 4.1 Compositions of alloy and composites

Materials	**Al**	**Cu**	**Mn**	**Mg**	**Fe**	**TiC**
Aluminium alloy	94 %	4	0.5	0.5	1	---
(Al alloy)-5TiC	Dispersion of TiC in the melt					5
(Al alloy)-10TiC						10

4.2 Density and Hardness Measurement

Utilizing the water displacement method, the density of the specimens was determined. A very accurate Mettler microbalance was used, which can record sample weights with an accuracy of about 10-5g. A Vickers hardness testing equipment was used to apply a force of 5 kg to the samples in order to evaluate their bulk hardness (as shown in Fig. 4.3). Diamond pyramid indenters were used to measure the hardness.

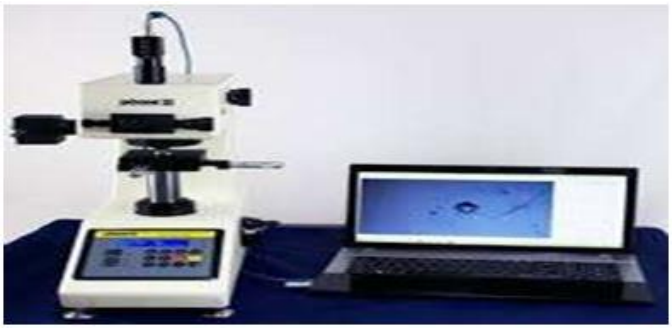

Figure 4.3 Vickers Hardne

4.3 Wear Tests

As test specimens for wear, cylindrical pins with 10 mm diameter and 30 mm length were manufactured. As shown in Figure 4.4, a pin-on-disc machine was used to conduct the wear testing. Emery paper with tightly bound SiC particles was wrapped around the disc with double- sided adhesive tape to form the abrasive medium. The 320-grit abrasive medium used has a 46 µm abrasive particle size, which corresponds to the 320 grit size of the abrasive medium. A cantilever mechanism was used to load the samples against the abrasive media. A normal load of 10 to 30 N, sliding velocities of 1 and 2 m/s, and a total sliding distance of 100 to 500 m were all included in the test settings The pins were cleaned in an acetone-filled ultrasonic bath both prior to and subsequent to each test, and then they were dried. The weight difference between the pin specimens before and after the tests

was measured to establish the wear loss, and this number was used to calculate the wear rate. A Mettler microbalance with a precision level of 0.01 mg was used to weigh the samples. During the testing, a chromel-alumel thermocouple was put into a hole close to the contacting surface to measure the temperature near the surface of the specimens. A friction transducer was used to quantify the friction force that was felt during wear testing, and this force was then transformed into the friction coefficient.

Figure 4.4 Pin-on-Disc Wear Test Machine

V. RESULTS

The observations made throughout the research are described in this chapter. This includes looking at the samples' microstructure and characteristics including hardness, density, and abrasive wear qualities. Investigations on the effects of changing loads, sliding distances, and abrasive size on abrasive wear response have been conducted. The factors of wear performance that have been researched include friction coefficient, wear rate, and frictional heating.

5.1 Microstructure

Prior to abrasion testing, the samples' microstructural characteristics are depicted in Figure 5.1. Primary dendrites were visible in the matrix alloy and were encircled by the eutectic (α+CuAl2) phase (Fig. 5.1a). The phases can be seen clearly in a magnified perspective (Fig. 5.1a). In addition, consisting TiC particles, Al-5TiC and Al-10-TiC composites had matrix characteristics that were the same as those of the matrix alloy (Fig. 5.1b and c). The matrix structure and distributed (submicron to 1-2 µm) TiC particles are shown in Figure 5.1b. Fig. 5.1c shows the bonding of the sound dispersoid and matrix.

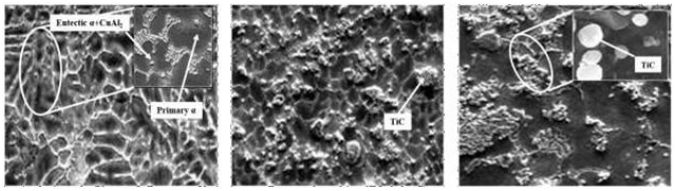

Figure 5.1 SEM morphological features of the (a) matrix Al alloy (b) Al-5TiC and (c) Al-10TiC composite

5.2 Density and Hardness

Table 5.1 shows the hardness and density of the samples. The incorporation of TiC particles led to higher hardness and density that increased further with the increasing concentration of TiC.

Table 5.1 Properties of the matrix alloy and composites

Materials	Density (g/cc)	Hardness (HV)
Al-2014 alloy	2.70	87
Al-2014-5wt % TiC	2.90	91
Al-2014-10 wt% TiC	2.95	95

5.3 Abrasive Wear Response

5.3.1Wear Rate

The wear rate of the samples evaluated over a continuous sliding distance of 500 m (known as test mode B), which corresponds to the final (5th) test period in test mode A, is shown in Fig. 5.4. It is clear that compared to the matrix alloy, the wear rate was lower when TiC particles were present. Additionally, a higher TiC content resulted in a bigger decline in the wear rate. Additionally, increasing the load caused the wear rate to increase, but test mode B had a lower wear rate than test mode A.

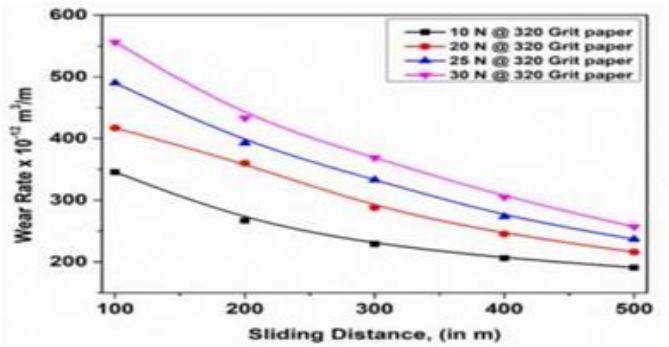

(a)

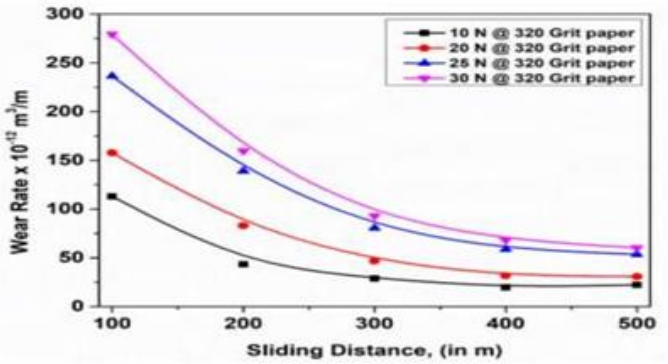

(b)

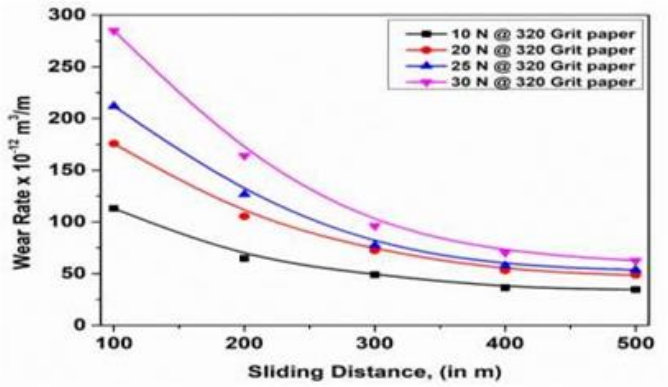

(c)

Figure 5.2 Wear rate as a function of sliding distance for (a) matrix Al alloy and (b) Al-5%TiC and (c) Al-10%TiC composites at different applied loads

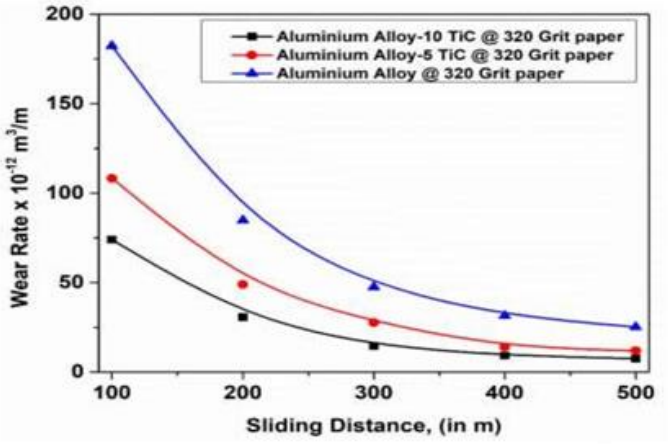

Figure 5.3 Wear behavior of the matrix Al alloy, Al-5%TiC and Al-10%TiC composites at an applied load of 20N

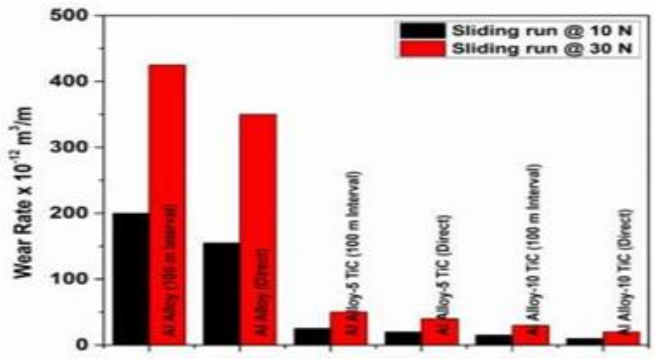

Figure 5.4 Wear rate of the matrix Al alloy, Al-5%TiC and Al-10%TiC composites tested for the sliding distance of 500 m run directly and in intervals of 100 m at typical applied loads of 10 & 30N against 320 grit abrasive particles

5.1.1 Frictional Heating

The temperature at the specimen surface for the matrix Al alloy, Al-5%TiC, and Al-10%TiC composites examined in test mode A is shown as a function of intermediate sliding distance in Fig. 5.5, specifically pertaining to the first and fifth (final) test intervals. A high initial rise in temperature was followed by a slower rate of rise until a steady state was reached. At greater loads and/or with coarser abrasive media, this trend was more pronounced. After reaching the apex, a drop in temperature was occasionally noted. Regardless of the kind of specimen material, the heating became more severe as the applied stress and abrasive particle size increased. In Figs. 5.6 and 5.7, the effect of TiC reinforcement on the frictional heating of the matrix alloy is depicted. The severity of frictional heating was lessened by the presence of TiC particles, and the severity of frictional heating was further diminished as the concentration of TiC rose. In comparison to the first test interval, the degree of warmth likewise decreased during the last test interval. At all loads tested against both abrasive sizes, this tendency was seen for both the matrix alloy and composites.

In test mode B, with a sliding distance of 500 m against 320 grit abrasive, the temperature of the samples near their contacting surface is shown in Fig. 5.8 as a function of the intermediate sliding distance. The temperature increased first as the sliding distance decreased, then increased at a slower rate until the matrix Al alloy reached a steady state (Fig. 5.8a). For both Fig. 5.8b and 5.8c at longer distances, the frictional heating tended to decline after reaching the peak but before the steady state condition. When compared to the matrix alloy, frictional heating was lower in the composites, and it got even lower as the TiC content arises.

At applied loads of 10 and 30 N against 320 grit abrasive, Fig. 5.9 depicts the highest temperature rise along the contacting surface of the specimens tested for 500 m in both test modes A and B. Higher frictional heating was produced as the load was increased, and test mode B showed higher frictional heating than test mode A. In addition, the temperature of the composites was lower than that of the matrix alloy.

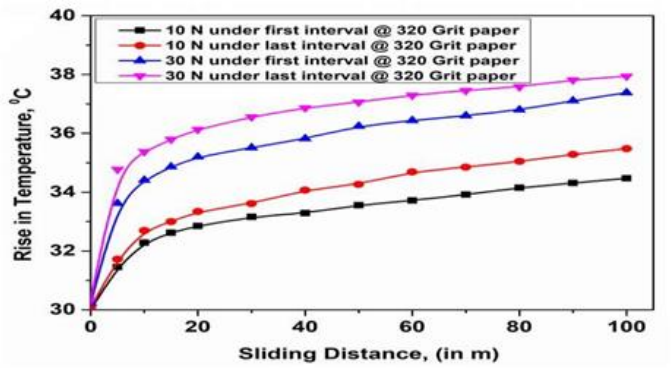

(a)

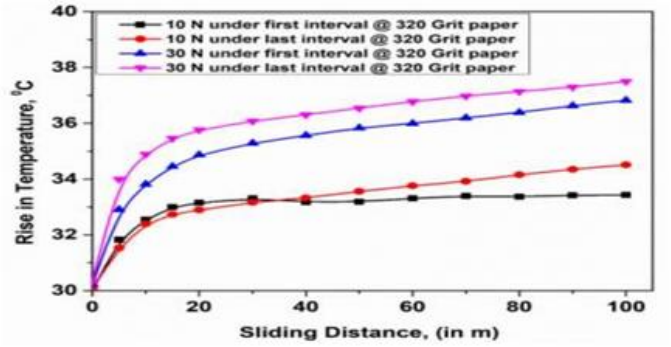

(b)

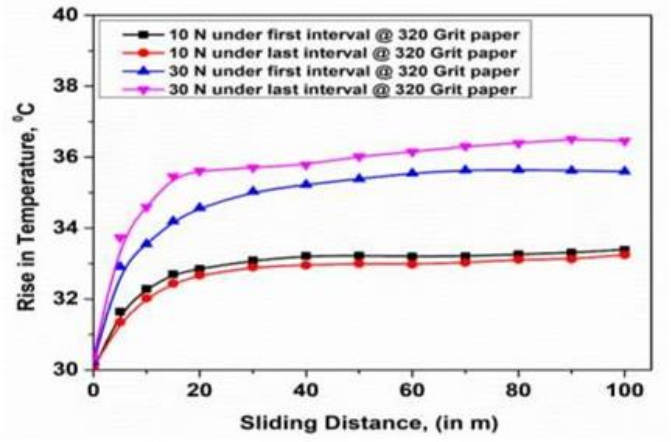

(c)

Figure 5.5 Temperature rise as a function of sliding distance in test mode A for the sliding distances of 100 and 500 m at an applied loads of 10 & 30N against 320 grit abrasive particles for
(a)matrix Al alloy, and (b) Al-5%TiC and (c) Al-10%TiC composites

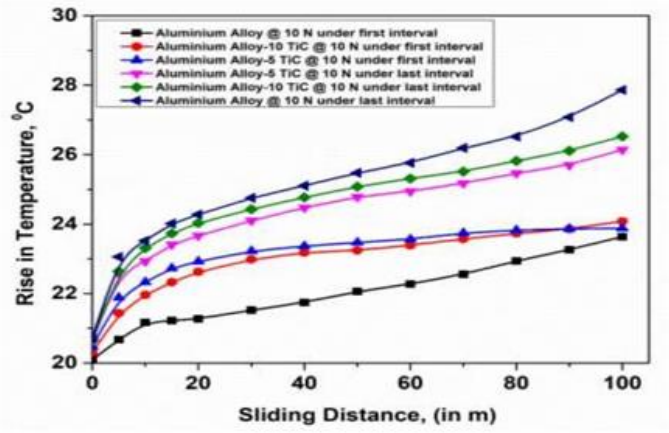

Figure 5.6 Temperature rise of the matrix Al alloy and Al-5&10%TiC composites plotted as a function of sliding distance for the samples tested for the 1st and 5th test intervals at an typical applied load of 10 N against 320 grit abrasive particles

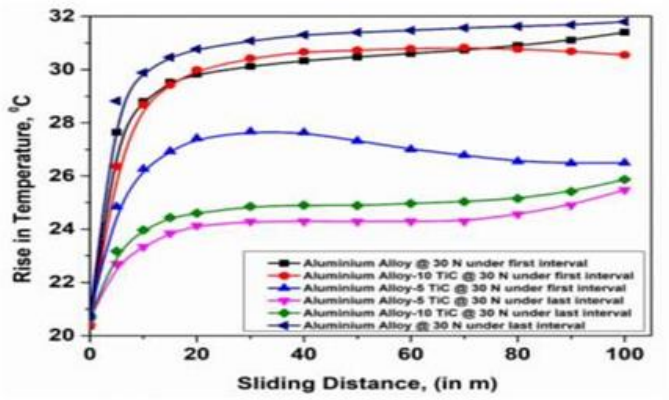

Figure 5.7 Temperature rise of the matrix Al alloy, Al-50%TiC and Al-10%TiC composites plotted as a function of sliding distance for the samples tested for the 1st and 5th test intervals at an applied load of 30 N against 320 grit abrasive particles

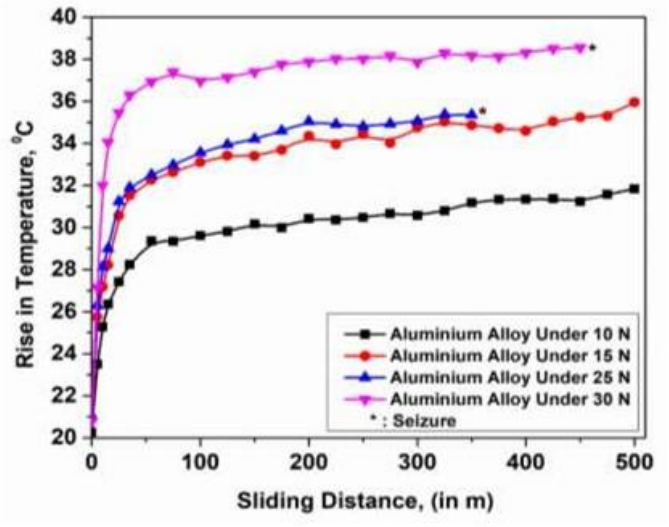

(a)

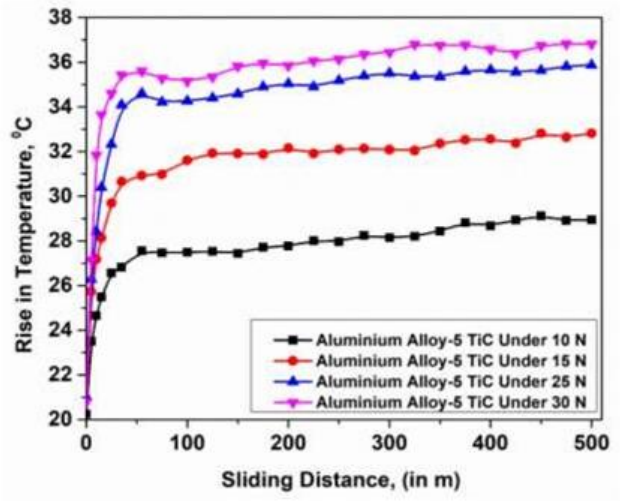

(b)

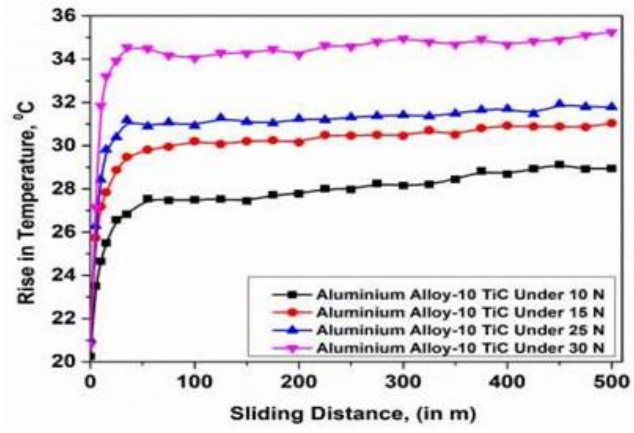

(c)

Figure 5.8 Temperature rise as a function of sliding distance of 500 m at different applied loads against 320 grit abrasive particles in case of the (a) matrix Al alloy, and (b) Al-5%TiC and (c) Al-10%TiC composites

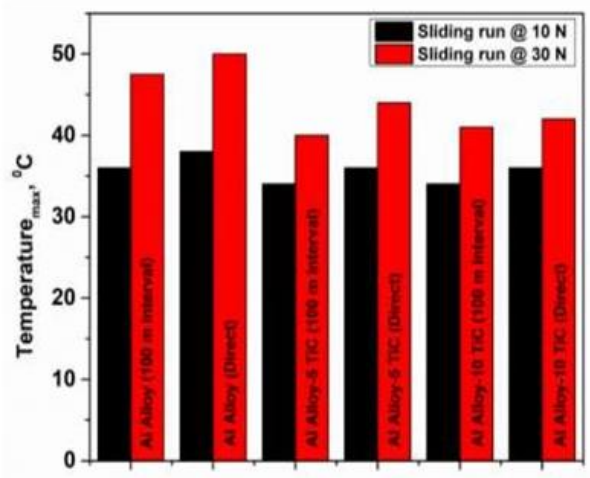

Figure 5.9 Maximum temperature in case of the matrix Al alloy and Al-5TiC & Al-5&10%TiC composites tested for the sliding distance of 500 m run directly in intervals of 100 m at an applied loads of 10 & 30N against 320 grit abrasive particles

5.1.2 Friction Coefficient

As a function of intermediate sliding distance at various applied loads, the friction coefficient of the matrix alloy and composites tested in test mode B is displayed in Fig. 5.13. With increasing applied stress, the friction coefficient dropped, and its behaviour with respect to sliding distance was comparable to that seen in test mode A. Additionally, compared to the matrix alloy, the composites showed decreased friction coefficients (Fig. 5.14). As the load increased, the friction coefficient likewise reduced. Fig. 5.15 compares the friction coefficients of the materials tested at 10 and 30 N load. The friction coefficient decreased as the load increased, and test mode B showed higher friction coefficients than test mode A.

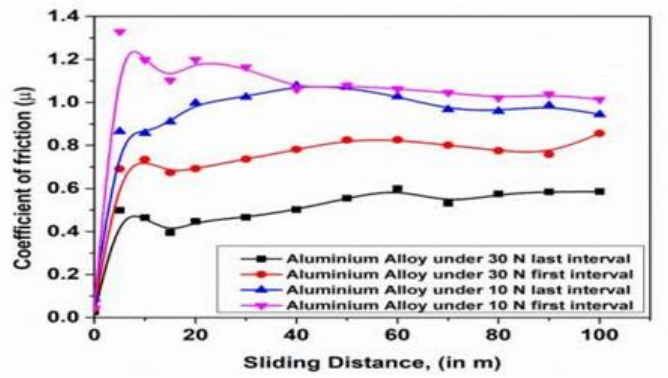

(a)

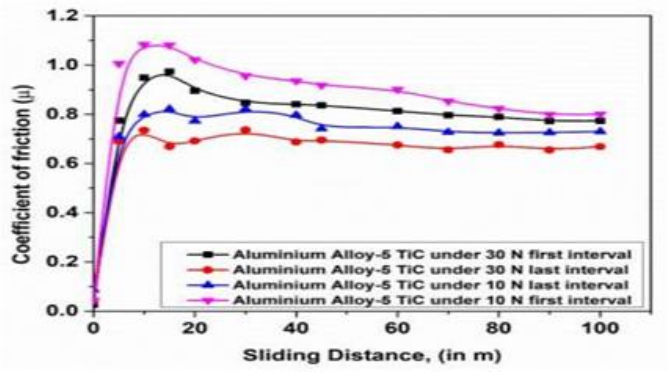

(b)

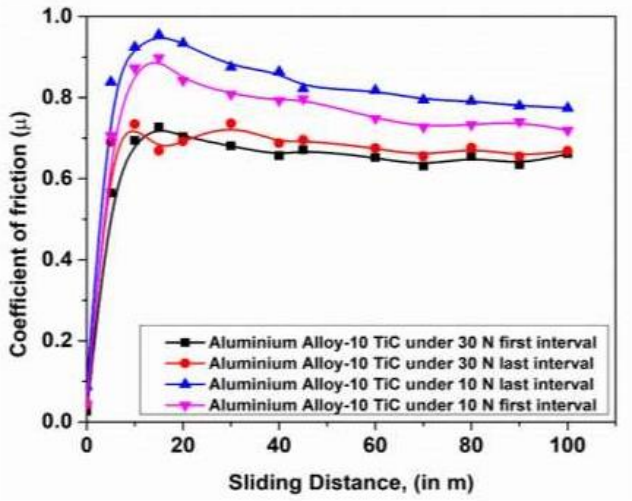

(c)

Figure 5.10 Friction coefficient plotted as a function of sliding distance for the sliding distances of 100 and 500 m at an applied loads of 10 and 30N against 320 grit abrasive particles in case of the (a) matrix Al alloy, and (b) Al- 5%TiC and (c) Al-10%TiC composites

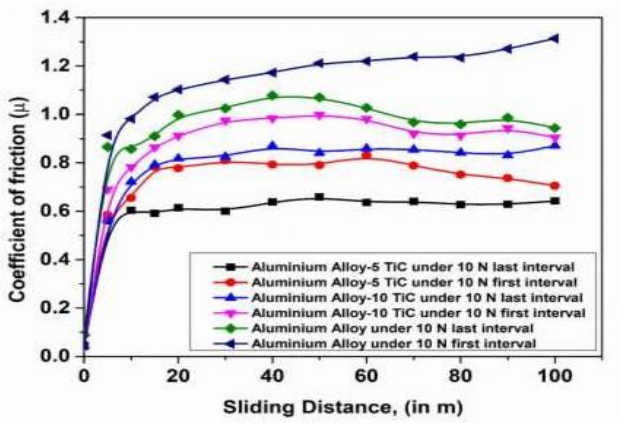

Figure 5.11 Frictional heating of the matrix Al alloy, Al-5TiC and Al-10%TiC composites plotted as a function of sliding distance for the samples tested for the 1st and last (5th) test intervals at an applied load of 10 N against 320 and grit abrasive particles

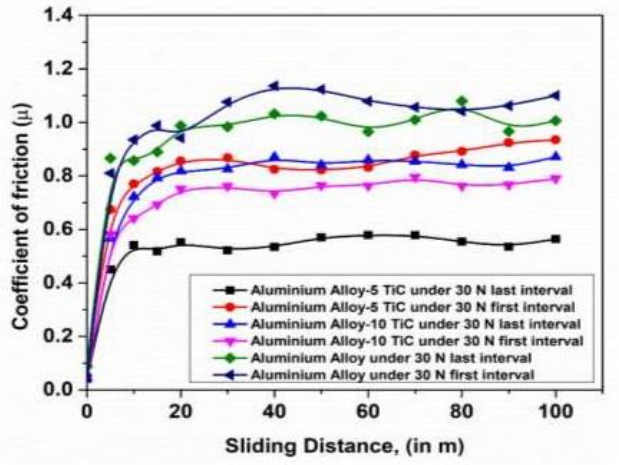

Figure 5.12 Friction coefficient of the matrix Al alloy, Al-5TiC and Al-5&10%TiC composites plotted as a function of sliding distance for the samples tested for the 1st and last (5th) test intervals at a typical applied load of 30 N against 320 grit abrasive particles

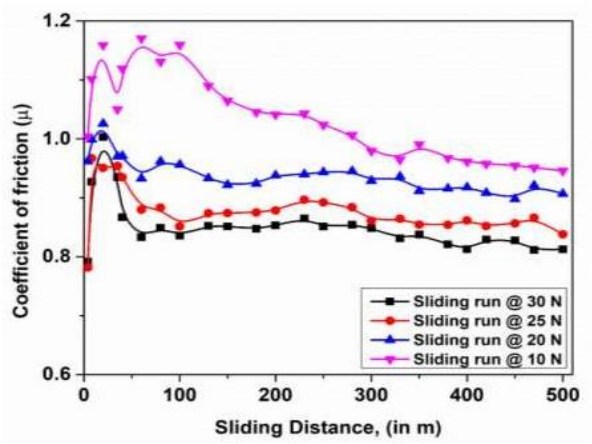

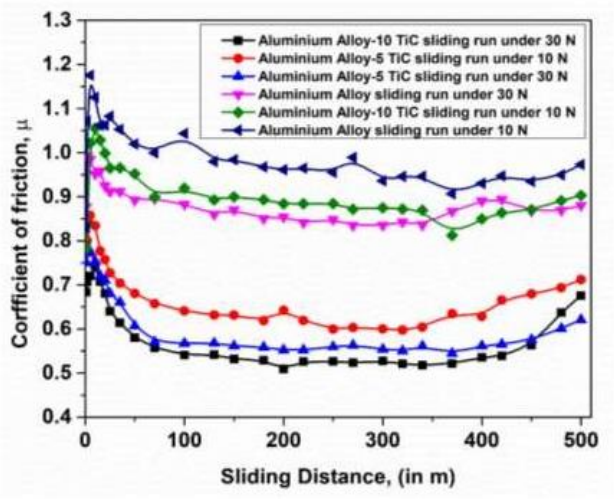

Figure 5.14 F riction coefficient plotted as a function of sliding distance for the matrix Al alloy, Al-5TiC and Al-5&10%TiC composites tested for the sliding distance of 500 m at an applied loads of 10 and 30 N against 320 grit abrasive particles

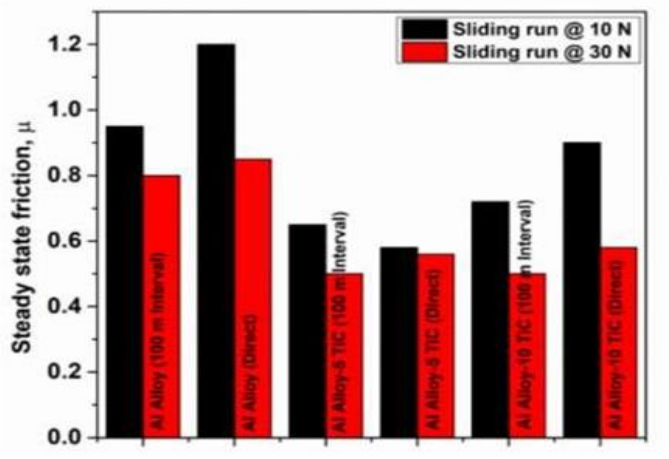

Figure 5.15 Steady state friction coefficient in case of the matrix Al alloy, Al-5%TiC and Al- 10%TiC composites tested for the sliding distance of 500 m run directly and in intervals of 100 m at an applied loads of 10 & 30N against 320 grit abrasive particles

VI. DISCUSSION

The observations made in this study are thoroughly discussed in this chapter, which also makes an effort to analyse them in relation to the unique nature and properties of the micro constituents found in the specimen material system and the underlying material mechanisms that control cutting efficiency and abrasive particle damage.

The predominant phase of the specimen material system's micro components is a solid solution of Cu in Al. The soft and ductile characteristic of this phase allows it to accommodate other hard and brittle micro components like Cu-Al and Fe-Al. While the soft phase holds them in place, the hard and ductile phases help with load-bearing. The greater hardness of the composites relative to the matrix alloy is proof that the addition of TiC particles to the matrix alloy improves the load- bearing capabilities. Thermal stability is aided by the strong melting properties of the micro components. Hard, brittle, and thermally stable phases enhance performance in terms of abrasive wear resistance by preventing abrasive particles from penetrating and carrying load, protecting the material.

The primary impacts of capping, clogging, attrition of abrasive particles, and subsurface work hardening of the specimen material are responsible for the decrease in wear rate of the samples with increasing sliding distance. The greater penetration that the abrasive particles achieve into the specimen surface is what causes the wear rate to increase with increased abrasive size and load. The relative higher degree of material softening in test mode B, which allowed for larger abrasive particle penetration depth, may be the cause of the higher wear severity found in test mode B compared to test mode A. Due to these particles' resistance to abrasive penetrating, the wear rate of the samples with TiC particle reinforcement was reduced. The rapid work hardening and abrasive action on the initially projecting asperities, which later undergo fragmentation, can be blamed for the initially high rate of temperature increase with increasing sliding distance. The wear state gets milder when more asperities make contact and distribute the load, which lowers the rate at which frictional heat is produced. Due to the TiC reinforcement's resistance to abrasive particle penetration, frictional heat generation in composites is lower than it is in matrix alloys. The same parameters regulate friction coefficient and frictional heating, as seen by the identical effects of sliding distance and abrasive size on the friction coefficient.

Despite a higher wear rate, the decrease in friction coefficient with increased load shows that these two metrics cannot be directly associated. While a deeper cut at a higher load can enhance wear rates, the resulting increase in frictional heat might also create a disproportionately greater amount of material softening, lowering the friction coefficient.

Overall, the findings of this investigation strongly imply that a variety of material- and test-related aspects affect the samples' wear performance, making it difficult to draw direct relationships. Therefore, to accurately determine if a material is suitable for use in actual applications, understanding the wear behaviour of materials should be tackled on a case-by-case basis.

VII. CONCLUSIONS

Observations made in this investigation lead us to draw the following conclusions:

1. The Al alloy matrix's microstructure showed primary dendrites and interdendritic areas made up of eutectic and CuAl2 phases. Phases that were abundant in Fe, Si, and Mg were also noticed. Along with the distinctive qualities of the matrix alloy, TiC particles were found in the composites. The composites' high interfacial adhesion between the dispersoid and matrix components was also noted.
2. Hardness and density were raised as a result of adding TiC particles to the matrix.
3. As the sliding distance grew, the specimens' abrasive wear resistance decreased, whereas the abrasive size and applied load had the reverse impact. In addition, test mode B showed a higher rate of wear than test mode A.

4. When the sliding distance was increased, it was found that the frictional heating increased quickly at first. But as time went on, the pace of growth reduced and eventually reached a stable state. Frictional heating was more prominent due to a higher applied load and bigger abrasive size. In addition, test mode B showed more frictional heating than test mode A.
5. Similar to frictional heating, it was discovered that the sliding distance, abrasive size, and test mode all had an impact on the friction coefficient; however, the applied load had the reverse effect.
6. Numerous aspects of the material itself as well as the testing settings have an impact on the wear behaviour of materials. However, the actual wear response is ultimately determined by the supremacy of some factors over others, which generates opposing influences. The complexity of the wear process results in a synergistic interaction between these variables. To evaluate a material's acceptability from a technical and application standpoint, it is necessary to acquire a systematic understanding of the wear response of materials on a case-by-case basis.

VIII. FUTURE SCOPE

The need to evaluate the wear behaviour of the material system in relation to variables like the type and morphology of the abrasive and reinforcement phase, the morphology and content of the matrix micro-constituents, and a wider range of test conditions like environment, sliding distance, track radius, load, and test methodology is instead highlighted. A thorough research of the worn surfaces, subsurface regions, and abrasive media is also necessary to support and validate the findings, making it possible to make more impactful claims and bringing the study closer to conclusion.

REFERENCES

[1] V.I. Nikitin, A.I. Chmelevskich, A.P. Amosov, A.G. Merzhanov, Book of Abstracts of the First International Symposium on SHS, Alma-Ata, Russian Federation,1991.
[2] K. C. Ramesh and R. Sagar, Int J Adv Manuf Technol, 15 (1999) pp 114–118
[3] Allison JE, Cole GS. JOM 1993;19.
[4] Rohatgi PK. Cast aluminium matrix composites for automotive applications. JOM 1991;10– 15.
[5] Doychak J. JOM 1992;46.
[6] Gibson PR, Clegg AJ, Das AA. Production and evaluation of squeeze cast graphitic Al–Si alloy. Mater. Sci. Technol. 1985; 1:558–67.
[7] Dellis MA, Keastenrmans JP, Delannay F. The wear properties of aluminium alloy composite. Mater. Sci. Eng. A 1991; 135:253–7.
[8] Dinwoodie J. Automotive applications for MMCs based on short staple alumina fibres. SAE Technical Paper Series, Int. Con. Exp., Detroit, Michigan; 1987. pp. 23–27.
[9] Joshi SS, Ramakrishnan N, Sarathy D, Ramakrishnan P. Development of the technology for discontinuously reinforced aluminium composites. In: Integrated Design and Process Technology. The First World Conference on Integrated Design and Process Technology, Austin, vol. 1; 1995. p. 492–497.
[10] Kocazac MJ, Khatri SC, Allison JE, Bader MG. MMCs, for ground vehicle, aerospace and industrial applications. In: Suresh et al, editor. Fundamentals of Metal Matrix Composites. Guildford: Butterworth; 1993. p. 297.
[11] Chadwich GA, Heath PJ. Machining of metal matrix composites. Met. Mater. 1990;2-6:73– 6.
[12] Jagadeesh, G. V., and Srinivasu Gangi Setti. "A review on micromechanical methods for evaluation of mechanical behavior of particulate reinforced metal matrix composites." Journal of Materials Science 55 (2020): 9848-9882.
[13] Rubino, Felice, et al. "Marine application of fiber reinforced composites: A review." Journal of Marine Science and Engineering 8.1 (2020): 26.
[14] Sun, Jie, et al. "Mechanical and electrochemical performance of hybrid laminated structural composites with carbon fiber/solid electrolyte supercapacitor interleaves." Composites Science and Technology 196 (2020): 108234.
[15] Singh, Lokesh, Bharat Singh, and Kuldeep K. Saxena. "Manufacturing techniques for metal matrix composites (MMC): an overview." Advances in Materials and Processing Technologies 6.2 (2020): 441-457.
[16] Fattahi, Mehdi, et al. "Characterization of triplet Ti–TiB–TiC composites: Comparison of in- situ formation and ex-situ addition of TiC." Ceramics International 46.8 (2020): 11726-11734.
[17] Sharma, Daulat Kumar, Devang Mahant, and Gautam Upadhyay. "Manufacturing of metal matrix composites: A state of review." Materials Today: Proceedings 26 (2020): 506-519
[18] Li, Shufeng, et al. "Powder metallurgy Ti–TiC metal matrix composites prepared by in situ reactive processing of Ti-VGCFs system." Carbon 61 (2013): 216-228
[19] Singh, Lokesh, Bharat Singh, and Kuldeep K. Saxena. "Manufacturing techniques for metal matrix composites (MMC): an overview." Advances in Materials and Processing Technologies 6.2 (2020): 441-457.

[20] Kumar, Ashish, R. C. Singh, and Rajiv Chaudhary. "Recent progress in production of metal matrix composites by stir casting process: An overview." Materials Today: Proceedings 21 (2020): 1453-1457.

[21] Yang, Dexuan, et al. "Highly conductive wear resistant Cu/Ti 3 SiC 2 (TiC/SiC) co- continuous composites via vacuum infiltration process." Journal of Advanced Ceramics 9 (2020): 83-93.

[22] Chu, Yu-Ming, et al. "Investigation of nano powders influence on melting process within a storage unit." Journal of Molecular Liquids 318 (2020): 114321.

[23] Deuis, R. L., C. Subramanian, and J. M. Yellup. "Dry sliding wear of aluminium composites—a review." Composites science and technology 57.4 (1997): 415-435.

[24] Patel, Murlidhar, Sushanta Kumar Sahu, and Mukesh Kumar Singh. "Abrasive wear behavior of SiC particulate reinforced AA5052 metal matrix composite." Materials Today: Proceedings 33 (2020): 5586-5591.

[25] Singh, Raj Kumar, Amit Telang, and D. A. S. Satyabrata. "Microstructure, mechanical properties and two-body abrasive wear behaviour of hypereutectic Al—Si—SiC composite." Transactions of Nonferrous Metals Society of China 30.1 (2020): 65-75.

[26] Batra, N. K., Iti Dikshit, and Neera Batra. "Effect of dry sliding adhesive wear on woven carbon, aramid and glass fabric polyetherimide (PEI) reinforced composite." J Crit Rev 7 (2020): 1812-1819.

[27] V. R, Arun Prakash, Jayaseelan V, and Melvin Victor Depoures. "Effect of silicon coupling

[28] grafted ferric oxide and e-glass fibre in thermal stability, wear and tensile fatigue behaviour of epoxy hybrid composite." Silicon 12 (2020): 2533-2544.

[29] Saber, D., et al. "Corrosive wear of alumina particles reinforced Al–Si alloy composites." Physics of Metals and Metallography 121 (2020): 188-194.

[30] Patel, Murlidhar, et al. "Abrasive, erosive and corrosive wear in slurry pumps–A review." Int. Res. J. Eng. Technol 7.3 (2020): 2188-2195.

[31] Kumar, M. Senthil, et al. "Experimental investigations on mechanical and microstructural properties of Al2O3/SiC reinforced hybrid metal matrix composite." IOP Conference Series: Materials Science and Engineering. Vol. 402. No. 1. IOP Publishing, 2018.

[32] Rakesh, Merugu, et al. "Role of in Situ Aluminide (Al3zr+ Al3ti) Particles on Nucleation Behavior of Aluminium Metal Matrix Composites." Available at SSRN 4280855.

[33] Ramnath, B. Vijaya, et al. "Aluminium metal matrix composites–a review." Rev. Adv. Mater. Sci 38.5 (2014): 55-60.

[34] Aatthisugan, I., A. Razal Rose, and D. Selwyn Jebadurai. "Mechanical and wear behaviour of AZ91D magnesium matrix hybrid composite reinforced with boron carbide and graphite." Journal of magnesium and alloys 5.1 (2017): 20-25.

[35] Yadav, Manoj Kumar, et al. "The study of mechanical and metallographic properties of friction stir processed AMMCs using different reinforcement." Materials Today: Proceedings 62 (2022): 283-292.

[36] Kannan, C., and R. Ramanujam. "Comparative study on the mechanical and microstructural characterisation of AA 7075 nano and hybrid nanocomposites produced by stir and squeeze casting." Journal of advanced research 8.4 (2017): 309-319.

[37] Chang, Hsiao-Lan, and Wei-Heng Shih. "Synthesis of zeolites A and X from fly ashes and their ion-exchange behavior with cobalt ions." Industrial & Engineering Chemistry Research 39.11 (2000): 4185-4191.

[38] Junqani, Mohammadreza Tamizi, Hamid Reza Madaah Hosseini, and Abolfazl Azarniya. "Comprehensive structural and mechanical characterization of in-situ Al–Al3Ti nanocomposite modified by heat treatment." Materials Science and Engineering: A 785 (2020): 139351.

[39] Raghavendra, N., and V. S. Ramamurthy, Tribological characterization of particulate mmc developed by stir casting process.